



# High-precision Penning-trap mass spectrometry for neutrino physics

Sergey Eliseev<sup>1,a</sup>, Yuri Novikov<sup>2,3</sup>

<sup>1</sup> Max-Planck institute for nuclear physics, 69117 Heidelberg, Germany

<sup>2</sup> Kurchatov Institute-PNPI, 188300 Gatchina, Russia

<sup>3</sup> Saint Petersburg state university, 199034 Saint Petersburg, Russia

Received: 27 October 2022 / Accepted: 2 February 2023

© The Author(s) 2023

Communicated by Nicolas Alamanos

**Abstract** After several decades of a dramatic development Penning-trap mass spectrometry now demonstrates unprecedented precision and sensitivity in measurements of the masses of a broad range of nuclides for various aspects of fundamental physics. This article reviews one facet of such mass measurements—a contribution of Penning-trap mass spectrometry to experiments on studies of neutrinos. These studies encompass the determination of the neutrino mass, the search for sterile and relic neutrinos and the search for neutrinoless double electron capture in order to determine the type of neutrinos as well as to check the conservation law of the total lepton number.

## Introduction: Neutrino physics—an area beyond the Standard Model

This review article is devoted to highly accurate measurements carried out by means of Penning-trap mass spectrometry (PTMS) for one of the challenging problems of modern physics—neutrino physics. The study of the properties of these mysterious particles is at the forefront of science [5]. Due to the extreme smallness of their masses (more than  $10^6$  times smaller than the electron mass), such a study has to inevitably be based on various experimental techniques that have to demonstrate unprecedentedly high sensitivity and accuracy. PTMS belongs to a pool of such techniques [9]. Moreover, this is the only technique that is capable of providing the neutrino studies with precisely enough measured mass differences and mass ratios of relevant nuclides.

PTMS has become an important and indispensable player in fundamental physics [7,9]. The success of this method in measuring masses of a wide range of nuclides—from ele-

mentary particles to superheavy chemical elements—is facilitated by a combination of three unconditional advantages. First, PTMS deals with ions which are almost at rest, i.e. at ultra-low energy. Second, PTMS possesses an unsurpassed sensitivity originated from the ability to perform measurements with just a single ion. Third, PTMS demonstrates a very high precision, superior to all other mass spectrometry methods.

PTMS is widely employed to test the Standard Model (SM) by contributing to a determination of fundamental constants, a test of quantum-electrodynamics (QED), quantum-chromodynamics (QCD), the CPT-invariance theorem, CP- and CVC-principles and by addressing various problems of neutrino physics [7].

Neutrinos, which are included in the SM as massless particles, literally made a crack in the strength and harmony of this model, achieved in recent decades. This arose from the proof of a non-zero neutrino rest mass. Moreover, at present the increasing search for new physics beyond the SM in many respects is associated with the basic neutrino properties, some of which are still entirely unknown [73]. The following list shows some open problems in neutrino physics:

- absolute scale of the neutrino masses,
- neutrino mass hierarchy,
- existence of eV- and keV- sterile neutrinos,
- the number of neutrino generations,
- violation of the total lepton number,
- the existence of right-handed heavy neutrinos,
- Majorana or Dirac nature of neutrinos.

Some of these open problems can be addressed by experiments that study nuclear processes that involve low-energy neutrinos (nuclear beta and double-beta decays) [21,27]. PTMS can assist these experiments with a precise determi-

<sup>a</sup> e-mail: sergey.eliseev@mpi-hd.mpg.de (corresponding author)

**Table 1** Minimum precision of PTMS needed for different problems of neutrino physics. Absolute precisions are given for a mass value  $A$  of 100

Problem	Relative mass precision	Absolute mass precision
Neutrino oscillation length	$10^{-8}$	$1 \text{ keV}/c^2$
Sterile keV neutrino	$10^{-9}$	$0.1 \text{ keV}/c^2$
Effective Majorana neutrino mass	$10^{-9}$	$0.1 \text{ keV}/c^2$
Relic neutrino	$10^{-10}$	$10 \text{ eV}/c^2$
Neutrino mass	$10^{-11}$	$1 \text{ eV}/c^2$

nation of the decay energies ( $Q$  values) of these processes by measuring the mass differences of decay nuclides.

This article briefly summarizes the latest achievements of PTMS in neutrino physics with the focus on its contribution to the determination of the neutrino mass and to a study of neutrinoless double-beta processes.

### Required uncertainties in the determination of the $Q$ values of beta and double-beta processes relevant to neutrino physics

Nuclear single beta processes such as  $\beta^-$  decay and electron capture (EC) are accompanied by an emission of neutrinos. The total energy carried away by the emitted neutrinos is defined by the total decay energy (i.e. mass difference of the mother and daughter nuclides,  $Q$  value of the decay). For  $\beta^-$  decay the neutrino-energy spectrum is continuous, whereas electron capture yields a neutrino-energy spectrum with characteristic peaks which correspond to the binding energies of various captured electrons. The uncertainty in the neutrino-energy determination is thus defined to large extent by the uncertainty of the atomic mass difference of the decay nuclides. In the case of double-beta processes only their neutrinoless mode is of particular interest [22]. Here, the uncertainty of the atomic mass difference of the decay nuclides defines the uncertainty in the determination of the half-life of the decay and hence of the effective Majorana neutrino mass.

How precisely one has to measure mass differences  $\Delta M$  of the decay nuclides depends on the particular goal (Table 1):

- Measurements related to the absolute neutrino mass determination require fractional uncertainties  $\delta(\Delta M)/M$  at the level smaller than  $10^{-11}$ , where  $M$  is the mass of the decaying nuclide. Such fractional uncertainties correspond to absolute uncertainties of a few ten meV/ $c^2$  to about one eV/ $c^2$  depending on the masses of the decaying nuclides.
- For the study of neutrinoless double-electron capture uncertainties at the level of  $1\text{--}10 \text{ eV}/c^2$  seem quite reasonable presently, because similar values are typically attributed to the widths of the intermediate levels in

double-electron capture, which govern the resonance enhancement of the probability of the neutrinoless mode of double-electron capture.

- One of the goals of neutrino oscillometry is a measurement of the oscillation length of neutrinos emitted in electron capture. This length depends on the neutrino energy and hence on the mass difference of the decay nuclides. A spatial resolution of liquid scintillator neutrino detectors employed in neutrino oscillation measurements [51, 71] requires to know the neutrino energy at the level of 100 eV.
- In the search for keV-sterile neutrinos the ratio of the capture probabilities from different atomic electron orbits is sensitive to the existence of sterile neutrinos. This ratio contains the total decay energy, which must be determined with an accuracy of better than 100 eV.
- Relic neutrinos, not yet observed, can be detected in a resonant absorption of antineutrinos by a nucleus during orbital electron capture [67]. Such a resonant absorption becomes possible when the atomic mass difference of parent and daughter decay nuclides is equal to the binding energy of the captured electron in the daughter nuclide. Here, an uncertainty of  $\Delta M$  at the level of 10 eV is required.

### PTMS—the best approach for direct precise mass measurements of nuclides

#### Ion motion in a Penning trap

The basic principle that underlies Penning-trap mass spectrometry is a trapping of a charged particle (an ion) with mass  $m$  and charge  $q$  in a static, uniform magnetic field  $B$ . In such a magnetic field the ion is forced to perform in the radial plane that is perpendicular to the magnetic-field lines a circular motion (free cyclotron motion) with frequency (Fig. 1a)

$$\nu_c = \frac{1}{2\pi} \frac{q}{m} B. \quad (1)$$

This motion is termed “free”, because an ion in a pure homogeneous magnetic field can freely move along the magnetic field lines. Thus, the ion motion is not confined to a certain

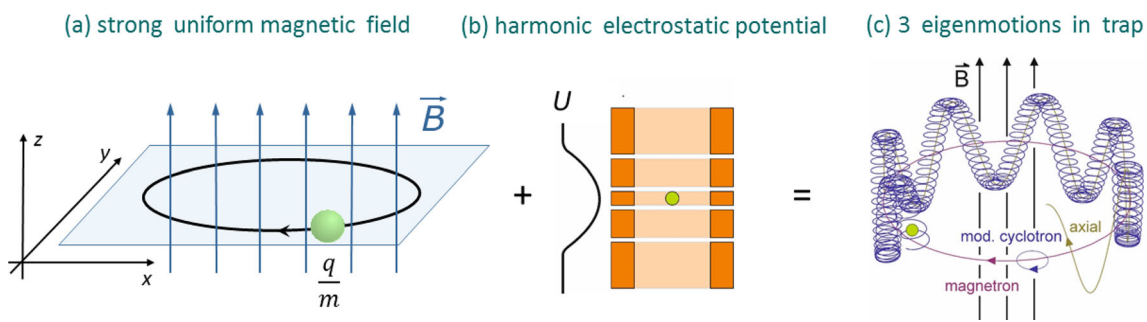


**Fig. 1** (a) A circular (free cyclotron) motion of a charged particle with mass  $m$  and charge  $q$  in a strong uniform magnetic field  $B$ . (b) A quadrupole (harmonic) electrostatic potential  $U$  created by, e.g., a stack of five cylindrical electrodes in order to confine the ion's motion

along the magnetic field lines. (c) Trajectories of the ion's eigenmotions in a Penning trap ( motional amplitudes are arbitrary and are not to scale)

volume. By measuring the ratio of the free cyclotron frequencies of two ions of interest one can directly determine the ratio of their masses. High-precision mass-ratio measurements imply the confinement of the ion's motion to a very small volume for up to several days. This is achieved by superimposing on the magnetic field a weak quadratic (harmonic) electrostatic potential in order to constrain the ion's motion along the magnetic field lines (Fig. 1b). A combination of two such fields is named the “Penning trap”. In experiments a static uniform magnetic field of several Tesla is usually generated by a superconducting solenoid that is operated in a persistent mode. An ideal quadratic electrostatic potential can be created by three electrodes—one ring electrode and two end-cap electrodes that are hyperboloids of revolution. Very often due to practical reasons a stack of five or seven cylindrical electrodes is used instead (Fig. 1b). In the Penning trap due to the presence of the electrostatic field the ion's motion differs from the free cyclotron motion. It can be treated as three independent trap motions: the axial motion, the trap cyclotron motion and the magnetron motion with frequencies  $\nu_z$ ,  $\nu_+$  and  $\nu_-$ , respectively (Fig. 1c).

The axial motion is an oscillation of the ion along the magnetic field lines in the harmonic potential well. The magnetron motion is a slow motion in the radial plane which is caused by a cross-product of the magnetic and electrostatic fields. The radial component of the electrostatic field also reduces the frequency of the cyclotron motion. The frequencies of the trap motions are given by ([12], pages 237–239 therein)

$$\nu_z = \frac{1}{2\pi} \sqrt{\frac{q}{m} \frac{U}{d^2}}, \nu_+ = \frac{1}{2} \left( \nu_c + \sqrt{\nu_c^2 - 2\nu_z^2} \right), \nu_- = \frac{1}{2} \left( \nu_c - \sqrt{\nu_c^2 - 2\nu_z^2} \right), \quad (2)$$

where  $d$  is the characteristic trap dimension ([12], pages 237 and 304 therein).

Neither the magnetron nor the trap cyclotron frequency is a simple function of the ion's mass and hence neither of these two frequencies alone can be used to determine the ion's mass with high precision. A measurement of the axial frequency could in principle be used for the determination of the ion's mass due to a simple relation between the axial frequency and the ion's mass. Nevertheless, impossibility to have a sufficiently stable electrostatic potential of the Penning trap over the entire measurement time rules out this option too.

The recipe for the determination of the free cyclotron frequency and hence the mass of an ion lies in measuring the frequencies of all trap motions with subsequent employment of the invariance theorem [11]

$$\nu_c^2 = \nu_+^2 + \nu_z^2 + \nu_-^2. \quad (3)$$

The invariance theorem holds true even for real Penning traps with such unavoidable imperfections as a misalignment of the magnetic-field and electrostatic-field axes and a certain ellipticity of the trap electrodes. In an ideal Penning trap a somewhat simpler expression for the free cyclotron frequency holds,

$$\nu_c = \nu_+ + \nu_-. \quad (4)$$

The sum frequency in Eq. (4) is named “side-band frequency” and is usually used in Penning-trap mass spectrometry of short-lived nuclides where mass ratios are rarely measured with fractional uncertainties of better than  $10^{-9}$  [33].

High-precision PTMS across the world

High-precision Penning-trap mass spectrometry naturally is divided into two subfields: (1) online PTMS of short-lived nuclides and (2) offline PTMS of long-lived and stable nuclides. The prefixes “online” and “offline” point to the pro-

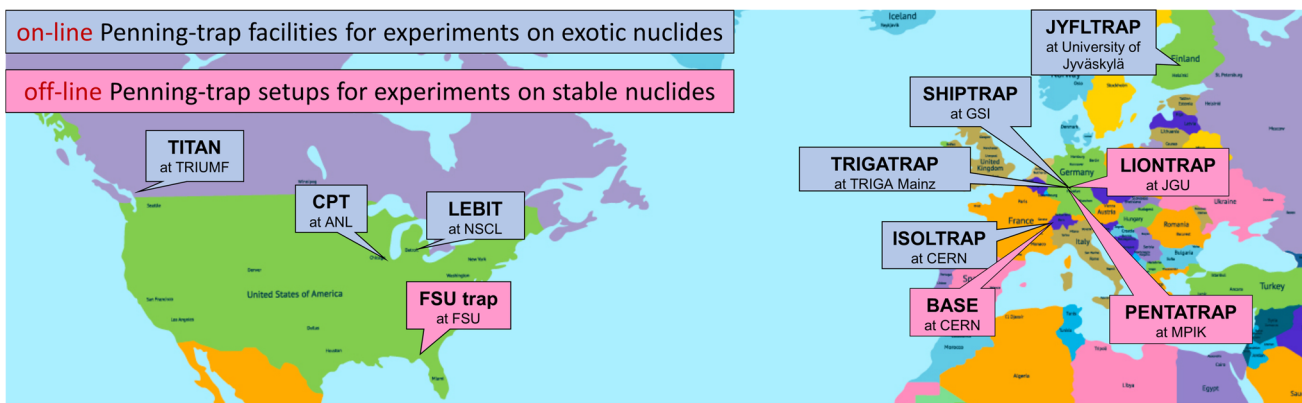


**Fig. 2** All operational high-precision Penning-trap facilities and their locations

duction mechanism of nuclides of interest. “Online” implies a production of short-lived nuclides at Rare Ion Beam (RIB) facilities in various nuclear reactions, whereas “offline” implies a production of ions with various ion sources from samples of (virtually) stable nuclides present in nature or of long-lived nuclides that can be synthesized elsewhere and brought to the experiment site. There are eleven experiments that aim at high-precision Penning-trap mass measurements. They are scattered over Europe, USA and Canada (Fig. 2).

Seven of them (ISOLTRAP [42], SHIPTRAP [10,19], TRIGA-TRAP [41], JYFLTRAP [28], CPT [57], LEBIT [55] and TITAN [20]) constitute the group of online Penning-trap facilities. Their physics programs complement each other to very large extent, since they carry out mass measurements on short-lived nuclides produced in different nuclear reactions and hence they probe different regions of the nuclear chart. The remaining four Penning-trap experiments (LIONTRAP [39], BASE [62], FSU-trap [61] and PENTATRAP [54]) comprise the group of offline setups. They are tailored to perform mass measurements on specific long-lived and stable nuclides. The BASE experiment is situated at CERN’s antiproton decelerator and devoted to experiments on antiprotons (g-factor and mass of an antiproton). LIONTRAP focuses on mass measurements of light nuclides. The FSU-trap and PENTATRAP are more universal machines devoted to mass measurements on a wide range of nuclides.

These two groups of Penning-trap experiments significantly differ in techniques employed to reduce the amplitudes of the ion’s motions (to “cool” the ion’s motions) and to measure the frequencies of the ion’s motions. This difference is a consequence of substantially different requirements put on mass measurements of short-lived and long-lived nuclides. The online Penning-trap facilities perform measurements with a moderate fractional uncertainty of down to approximately  $10^{-8}$  of masses of short-lived nuclides synthesized with very low production rates. Thus, the main demand for ion-motions cooling and trap-frequencies measurement tech-

niques in such experiments is their fastness, relative simplicity and a single-ion sensitivity of the ion detection system at room temperature. The major goal of the offline Penning-trap setups are mass measurements on long-lived nuclides with extremely low fractional uncertainties of down to  $10^{-12}$ . In order to be able to reach such uncertainties it is mandatory to reduce the ion’s motion confinement volume to a few cubic micrometers. Despite such small ion’s motional amplitudes the frequency measurement techniques have to be sensitive enough to allow frequency measurements on just a single ion. Thus, the offline Penning-trap experiments are inevitably cryogenic with Penning traps kept at a temperature of approximately 4.2 K (temperature of liquid helium at normal atmospheric pressure).

#### Cyclotron-frequency measurement techniques

In online Penning-trap mass spectrometry a two-trap experimental scheme is predominant. The first trap (preparation or cooler trap) is filled with helium gas at a typical pressure of approximately  $10^{-4}$  mbar and serves for cooling the ion’s motions with the mass-selective buffer gas cooling technique [56]. The trap cyclotron and axial motions lose their energies through collisions with helium atoms until they reach within a few ten to hundred ms thermal equilibrium with helium gas. The magnetron motion is metastable. Its interaction with helium gas results in an increase of its radius. The cooling of the magnetron motion is accomplished by its coupling to the cyclotron motion by means of a quadrupole rf field at the side-band frequency of the ion of interest. Thus, this cooling technique is mass-selective making the cooler trap additionally a mass separator with a typical resolving power of about  $10^5$ . A “cooled” ion has the radii of the radial motions of approximately 0.1 mm and the amplitude of the axial motion of about 1 mm. After cooling the ion is transported to the second trap (measurement trap) where a measurement of its trap-motion frequencies takes place with

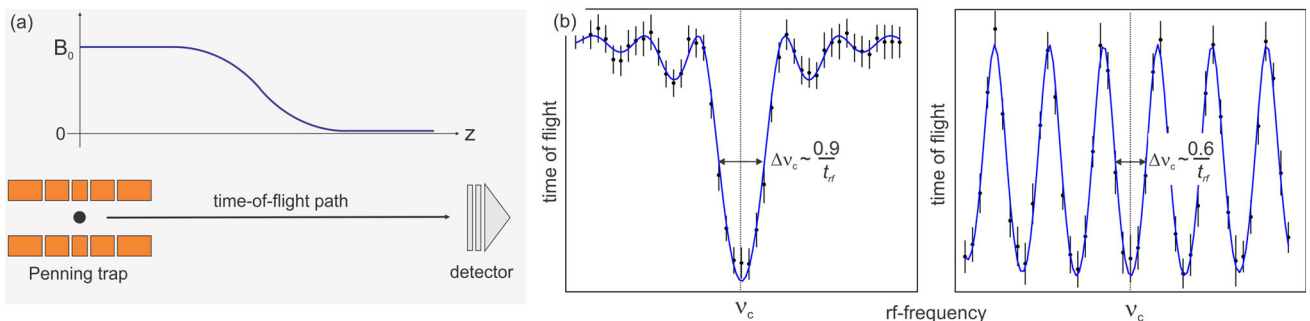


**Fig. 3** (a) A sketch of the Time-of-Flight Ion-Cyclotron-Resonance technique. (b) Time-of-Flight (ToF) resonances. The left and right ToF resonances are obtained with a single rf-pulse and a two rf-pulse (Ramsey) excitation schemes, respectively. The black points with uncertain-

ties are experimental data, the blue curves are model functions fit to the experimental points [43, 44].  $t_{rf}$ —duration of the rf excitation—defines the resolving power of the technique

two frequency-measurement techniques: (1) Time-of-Flight Ion Cyclotron Resonance (ToF-ICR) [38] and Phase-Imaging Ion Cyclotron Resonance (PI-ICR) [24, 25] techniques. The determination of the cyclotron frequency with the ToF-ICR is based on a measurement of the time of flight of an ion between the Penning trap and an ion-counting detector (usually a microchannel-plate (MCP) detector) that is placed on the axis of the trap in a weak magnetic field (Fig. 3a).

An ion in the Penning trap possesses an orbital magnetic moment  $\vec{\mu}$  that is given by

$$|\vec{\mu}| = |\pi \cdot q \cdot (r_+^2 v_+ + r_-^2 v_-)|, \quad (5)$$

where  $r_-$  and  $r_+$  are the magnetron-motion and the cyclotron-motion radii, respectively. The ion ejected from the trap toward the MCP detector passes a region with a gradient of the magnetic field  $\partial \vec{B} / \partial z$ , in which the ion is exposed to an accelerating force  $\vec{F}$  which is given by

$$|\vec{F}| = |\vec{\mu} \cdot \frac{\partial \vec{B}}{\partial z}|. \quad (6)$$

Thus, the time of flight of an ion from the trap to the MCP detector depends on the radii of the ion magnetron and cyclotron motions. The radii can be altered in various ways through exerting on the ion radio-frequency (rf) fields of various multipolarities and temporal profiles at certain frequencies. In order to determine the cyclotron frequency of an ion a sequential combination of a dipole rf field at the magnetron frequency and a quadrupole rf field at a frequency close to the side-band frequency is exerted on the ion. By varying the frequency of the quadrupole rf field one can obtain a so-called time-of-flight resonance (ToF resonance)—the dependence of the time of flight of the ion on the frequency of the quadrupole rf field exerted on the ion (Fig. 3b). The shape of the ToF resonance depends on the temporal profile of the quadrupole rf field. By fitting to the experimental ToF reso-

nance a corresponding model function [43, 44] one can determine the side-band frequency and hence the mass of the ion.

The PI-ICR technique is based on a measurement of the phases of the magnetron and cyclotron motions that are accumulated in a certain well defined phase-accumulation time  $t_{phase}$ . The phase of the corresponding ion radial motion is derived from the position of the ion in the trap with respect to the trap center for different phase-accumulation times (Fig. 4). The position of the ion in the trap is projected with a certain amplification factor onto a position-sensitive MCP detector. The ion position on the detector is defined by two polar coordinates: the distance  $R$  with respect to the image of the trap center (radial position) and the angle  $\phi$  with respect to an arbitrarily chosen polar axis (angular position). Two angular positions  $\phi_1$  and  $\phi_2$  that correspond to two phase-accumulation times  $t_{phase_1}$  and  $t_{phase_2}$ , respectively, yield the frequency  $v_{radial}$  of the corresponding radial motion according to

$$v_{radial} = \frac{(\phi_2 - \phi_1) + 2\pi n}{2\pi(t_{phase_2} - t_{phase_1})}, \quad (7)$$

where  $n$  is the number of revolutions the ion performs in time  $t_{phase_2} - t_{phase_1}$ .

Compared to the ToF-ICR, the PI-ICR technique offers a gain of approximately 5 in the precision of the side-band frequency determination and a gain of about 40 in the resolving power.

The virtue of both techniques is its sensitivity to a single ion achieved at a room temperature. A substantial drawback of the techniques is the necessity to have at least a few ten ions to acquire a ToF resonance or a phase image. This is the major limiting factor of these techniques for mass measurements on nuclides synthesized with extremely low production rates. In this respect, the record is held by SHIPTRAP with its measurement of the mass of  $^{257}\text{Rf}$  which was delivered to

**Fig. 4** A basic principle of the Phase-Imaging Ion-Cyclotron-Resonance technique (the different parts of the figure are not to scale). The frequency of the ion's radial motion is determined from the projection of the ion's position in the trap at different times onto a position-sensitive MCP detector. For more details see the text

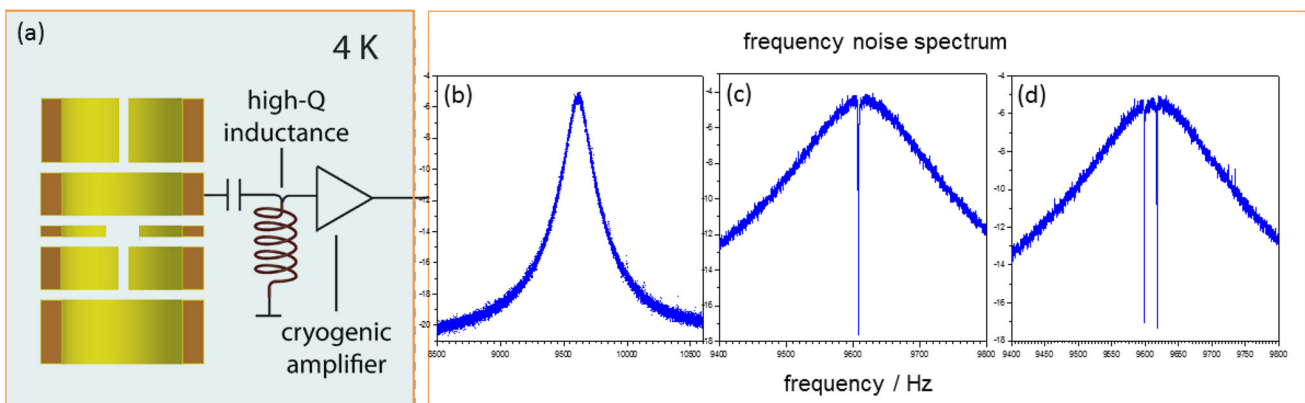
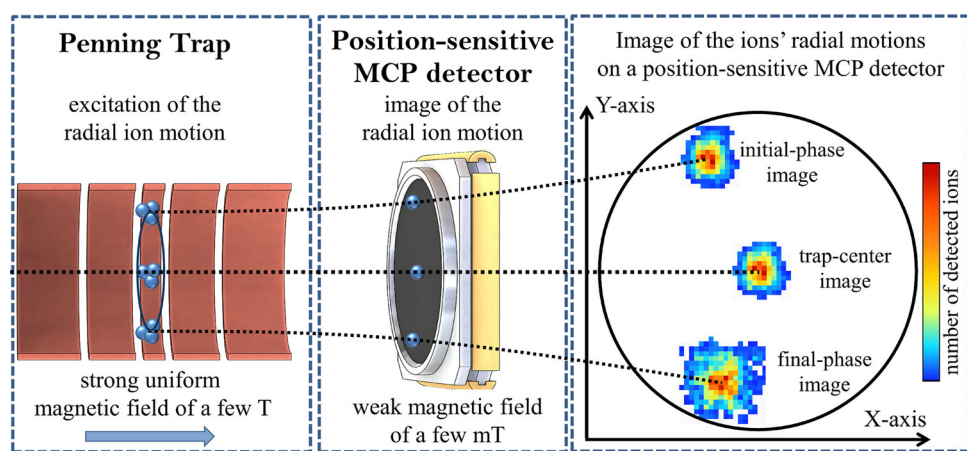


**Fig. 5** (a) A schematic representation of a LCR resonant tank that is employed for reducing the ion's motional amplitudes and for measuring the frequencies of the ion's eigenmotions. (b) A noise amplitude spectrum of a LCR resonant tank in the frequency domain. (c) A noise spectrum of a resonant tank with one of the ion's eigenmotions coupled

to the resonant tank. The coupled ion's motion shorts at its frequency the impedance of the resonant tank, thus resulting in an appearance of a dip. (d) A side-band coupling of another ion's eigenmotion to the eigenmotion coupled to the resonant tank splits the single dip into two dips. For more details see the text

the Penning trap with a rate of just one ion per day (paper in preparation).

In offline Penning-trap mass spectrometry of long-lived and stable nuclides ions of the nuclide of interest are usually available to mass measurements in a sufficiently large quantity. The major challenge in this case is the cooling of the ion's motion amplitudes to a few  $\mu\text{m}$  with a subsequent measurement of the ion's motion frequencies with extremely low uncertainties of down to a few parts in  $10^{12}$ . In order to make such high-precision frequency measurements feasible, an ion-motion cooling and a frequency measurement techniques based on the non-destructive detection of the image current induced by the ion motion in an external LCR resonant circuit (resonant tank) are employed. The electrodes of the Penning trap and the associated image-charge detection electronics are cooled to a temperature of liquid helium (about 4 K) to provide a single-ion sensitivity. The resonant tank is formed by the inductance of a superconducting inductor attached to one of the electrodes of the trap and by the par-

asitic capacitance of the trap electrode, the inductor and the wires that connect the inductor to the trap electrode (Fig. 5a).

The noise spectrum of the resonant tank in the frequency domain takes on the shape of a resonant curve (Fig. 5b). If the frequency of one of the ion's motions is close to the resonant frequency of the resonant tank, this ion's motion couples to the resonant tank. It means the ion's motion comes within a few ten to a few hundred ms through Coulomb interaction into thermal equilibrium with the electrons of the resonant tank. This technique is known as “resistive cooling” [70]. The “cooled” ion motion reveals itself in the frequency noise spectrum of the resonant tank as a dip with the minimum that corresponds to the frequency of the coupled ion's motion (Fig. 5c). Thus, a coupling of the ion's motion to the resonant tank also allows one to directly measure the frequency of the “cooled” ion motion (dip technique [70]). Usually, one cools in this way only the axial motion, since its frequency can be easily adjusted to the frequency of the resonant tank by varying the electrostatic potential of the trap. The radial motions

are cooled indirectly by their coupling to the axial motion by means of a quadrupole rf field at a sum or a difference of the frequencies of the coupled motions. The coupling splits the single dip into two dips (Fig. 5d) (double-dip technique [66]). By measuring the frequencies that correspond to the minima of two dips one can determine the frequency of the coupled radial motion. Thus, with the dip and double-dip techniques one can, first, reduce the amplitudes of all three ion's trap motions to few  $\mu\text{m}$  and, second, to measure their frequencies. Indeed, the dip and double-dip techniques are methods of choice to measure the frequencies of the axial and magnetron motions, respectively. The frequency of the trap cyclotron motion is usually measured with much faster Pulse-and-Phase (PnP) [15] or Pulse-and-Amplify (PnA) [63] techniques. The basic idea that underlies these techniques is very similar to that of the PI-ICR method. One determines the trap cyclotron frequency from the measurement of the phase accumulated by the trap cyclotron frequency in a well defined time  $t_{\text{phase}}$ . Here, one first excites the trap cyclotron motion to a radius of a few ten  $\mu\text{m}$  to set and measure its initial phase. After that the trap cyclotron motion freely evolves for  $t_{\text{phase}}$  with subsequent measurement of its final phase. The phases are measured by coupling the trap cyclotron motion to the axial motion with a quadrupole pulse of certain duration and amplitude ( $\pi$ -pulse [16]) at a sum (PnP) or a difference (PnA) of the trap cyclotron and axial frequencies. The  $\pi$ -pulse imprints the cyclotron-motion phase into the axial-motion phase. The coupling of the axial motion to the resonant tank allows for the readout of the axial-motion and hence cyclotron-motion phases.

### Mass-difference measurements for the determination of the electron (anti)neutrino mass in $\beta^-$ decay and electron capture

The three flavor eigenstates  $\nu_\alpha$  ( $\alpha = e, \mu$  and  $\tau$ ) of the neutrino in the SM are considered linear combinations of three neutrino mass eigenstates  $\nu_i$  ( $i = 1, 2, 3$ ) with masses,  $m_1$ ,  $m_2$  and  $m_3$ . The electron neutrino mass  $m_{\nu_e}$  is defined as

$$m_{\nu_e} = \sqrt{\sum_{i=1}^3 |U_{ei}|^2 m_i^2}, \quad (8)$$

where  $U_{ei}$  are the elements of the top row of the  $3 \times 3$  unitary leptonic mixing matrix. This electron neutrino mass is determined in experimental studies of  $\beta^-$  decay and electron capture. It approximately equals  $m_1$  regardless of the  $m_i$  ordering (normal or inverted) [32]. To date, an upper limit of about  $0.8 \text{ eV}/c^2$  on the electron antineutrino mass has been obtained from the study of the tritium  $\beta^-$  decay [1], whereas a substantially larger value for an upper limit on

the electron neutrino mass at the level of  $150 \text{ eV}/c^2$  has been yielded by the ECHo experiment within the first phase of the ECHo-1k from the analysis of the electron capture in  $^{163}\text{Ho}$  [35, 65]. There are two more experiments, still under construction, that also aim to determine the (anti)neutrino mass with an uncertainty of smaller than one  $\text{eV}/c^2$  [29, 46, 52]. In these experiments the (anti)neutrino mass value is determined from the analysis of either the atomic de-excitation spectrum of the electron capture in  $^{163}\text{Ho}$  or the the electron energy spectrum of the  $\beta^-$  decay of tritium. Regardless of the decay process, the analysis requires the knowledge of the  $Q$  value of the decay under investigation with a very low uncertainty. Presently two Penning-trap experiments, namely FSU-trap [48] and PENTATRAP [54] have in their measurement programme the determination of the  $Q$  values of these two beta processes.

### $\beta^-$ decay energy of tritium

Experiments on the determination of the antineutrino mass from the  $\beta^-$  decay of tritium have a long history dating back to the 40's of the past century. It is thus no surprise that the first direct high-precision determination of the  $Q$  value of this beta process was undertaken with Penning traps at the advent of high-precision Penning-trap mass spectrometry on nuclides in early 90's of the past century. Van Dyck at the University of Washington measured with his Penning-trap mass spectrometer the mass difference of tritium and  $^3\text{He}$  ( $\Delta M(\text{T}-^3\text{He})$ ) with an uncertainty of  $1.7 \text{ eV}/c^2$  utilizing a frequency-shift detector to observe cyclotron resonances [64]. Thirteen years later SMILETRAP slightly reduced the uncertainty of the  $\Delta M(\text{T}-^3\text{He})$  to  $1.2 \text{ eV}/c^2$  employing the ToF-ICR technique [49]. A breakthrough in the measurement of the  $\Delta M(\text{T}-^3\text{He})$  happened in 2015 when E. G. Myers with his FSU-trap decreased the uncertainty of the  $\Delta M(\text{T}-^3\text{He})$  by almost two orders of magnitude by employing the PnP technique on two ions simultaneously stored in the trap [48]. The obtained  $\Delta M(\text{T}-^3\text{He})$  value of  $18\,592.01(7) \text{ eV}/c^2$  is still unbeaten.

### Electron-capture decay energy of $^{163}\text{Ho}$

Few years ago, the electron capture in  $^{163}\text{Ho}$  began to be considered a real alternative to the  $\beta^-$  decay of tritium for the determination of the neutrino mass thanks to a rapid development of cryogenic microcalorimetry and based on this technique two experiments, ECHo [35, 65] and HOLMES [52]. With this development came the need in a direct precise determination of the  $Q$  value of this beta process. The first determination of the  $Q$  value of  $2833(33) \text{ eV}$  was carried out in 2015 with SHIPTRAP utilizing at that time the novel PI-ICR technique [26]. The reached uncertainty of approximately  $33 \text{ eV}$  allowed one to solve in favour of cryogenic microcalorime-

try the long-standing problem of large discrepancies in the  $Q$  value of the EC in  $^{163}\text{Ho}$  determined by different techniques.

The ECHo and HOLMES experiments are expected to determine the  $Q$  value from the analysis of the atomic microcalorimetric spectrum of the EC in  $^{163}\text{Ho}$  with an uncertainty of a few eV. Thus, an independent and direct determination of the  $Q$  value with Penning traps has to yield an uncertainty smaller than 1 eV in order that the ECHo and HOLMES experiments could use it in their calculations of the systematic uncertainty in the neutrino mass determination. PENTATRAP has recently accomplished this task by measuring with uncertainties smaller than  $5 \cdot 10^{-12}$  the cyclotron-frequency ratios of  $^{163}\text{Ho}$  and  $^{163}\text{Dy}$  ions in different charge states [58]. It has become feasible due to several unique features of PENTATRAP. First, the mass spectrometer of the PENTATRAP experiment has five cryogenic geometrically identical cylindrical Penning traps that are placed in the vertical cold bore of a 7-T persistent-mode superconducting magnet. The magnetic field is very stable demonstrating an almost linear relative drift of just  $10^{-10}/\text{h}$ . Second, the traps are biased by a high-stability voltage source Starep [13] that is an in-house development for PENTATRAP. The use of several Penning traps opens the door to the possibility to perform simultaneous measurements on several ions. Third, measurements are carried out on highly charged ions. Compared to measurements on low charged ions this substantially increases the precision of measurements of a cyclotron-frequency ratio of two ions. For instance, an approximately 12-h long measurement on  $^{163}\text{Ho}^{40+}$  and  $^{163}\text{Dy}^{40+}$  ions yields a statistical uncertainty of about  $6 \cdot 10^{-12}$  of their cyclotron-frequency ratio. Fourth, an EBIT ion source combined with a laser-desorption technique allows for a production of highly charged ions from solid samples that contain just a few nanograms of a nuclide of interest [59]. And finally, the mass spectrometer is placed in a dedicated temperature-stabilized room.

The measurement was carried out on pairs of  $^{163}\text{Ho}$  and  $^{163}\text{Dy}$  ions in three charge states (38+, 39+ and 40+) in order to rule out a potential shift of the cyclotron-frequency ratio due to a possible existence of an atomic metastable state in one of these ions [60]. In order to come from the measured cyclotron-frequency ratio to the required  $Q$  value, which is just the mass difference of neutral  $^{163}\text{Ho}$  and  $^{163}\text{Dy}$ , the binding energy differences of the missing electrons in  $^{163}\text{Ho}$  and  $^{163}\text{Dy}$  ions were computed by several methods with sub-eV uncertainties. The final uncertainty of the  $Q$  value of the EC in  $^{163}\text{Ho}$  does not exceed 1 eV [58].

#### $\beta^-$ decay energy of $^{187}\text{Re}$

Until about 20 years ago the  $\beta^-$  decay of  $^{187}\text{Re}$  was considered as promising as the  $\beta^-$  decay of tritium for the determination of the neutrino mass. This nuclear process

has the smallest  $Q$ -value of all  $\beta^-$  decays between the ground states and thus the analysis of its electron-energy spectrum was expected to have a very high sensitivity to the neutrino mass. Several experiments were set up to analyze the energy spectrum of the emitted electron by means of cryogenic microcalorimetry [3, 4, 17, 34]. Unfortunately, this activity had to be frozen due to several factors that severely hampered the development of experiments with  $^{187}\text{Re}$ . First,  $^{187}\text{Re}$  lives a few ten billion years that requires the use of large amount of  $^{187}\text{Re}$  in experiments in order to have a reasonably high decay rate. Second, rhenium becomes superconducting at temperatures of a few ten mK. This worsens the performance of cryogenic microcalorimetry. Finally, the  $\beta^-$  decay of  $^{187}\text{Re}$  is a unique first-forbidden  $\beta^-$  decay. A convenient way to plot the electron-energy spectrum of the  $\beta^-$  decay is the Kurie plot. For allowed transitions the Kurie plot is a straight line which intercept the  $x$  axis at the decay energy  $Q$ . If a particular  $\beta$  transition is forbidden, its Kurie plot departs from linearity. The exact shape of the Kurie plot depends on the degree of forbiddenness and is subject to model calculations, which complicate the analysis of the electron-energy spectrum. Nevertheless, the experiments with  $^{187}\text{Re}$  yielded a very valuable piece of information to PTMS. They determined the  $Q$  value of the  $\beta^-$  decay of  $^{187}\text{Re}$  with unprecedentedly small uncertainty of just 1.6 eV. This so-called cryogenic microcalorimetric  $Q$  value became a reference value for testing the accuracy of measurements with Penning traps. Moreover, it is not ruled out that a second chance might be given to this beta process in the future. If this happens, an independent and direct determination of the  $Q$  value with an uncertainty of about 1 eV will be demanded for the assessment of a systematic uncertainty in the neutrino mass determination from the analysis of the electron-energy spectrum of this beta process.

The history of measurements of the  $Q$  value of the  $\beta^-$  decay of  $^{187}\text{Re}$  with Penning traps is very similar to that of the EC in  $^{163}\text{Ho}$  described in the previous subsection. In 2014 it was determined with SHIPTRAP to be 2492(33) eV with an uncertainty of about 33 eV employing the PI-ICR technique [50] followed in 2018 by a substantially more accurate measurement of  $Q = 2470.9(13)$  eV with PENTATRAP with an uncertainty of 1.3 eV [31]. The  $Q$  values obtained with Penning traps are in good agreement with the cryogenic microcalorimetric  $Q$  value.

Search for new beta transitions suitable for a determination of the neutrino mass

There are several criteria that define the suitability of a particular beta transition for experiments on a determination of the neutrino mass. First, this is the magnitude of the  $Q$  value of the considered beta transition. Roughly speaking the smaller its  $Q$  value is, the more sensitive this beta transition is sup-

posed to be to the neutrino mass value. Second, the degree of forbiddenness is also a crucial factor that can render a beta transition with even a very small  $Q$  value unsuitable for the determination of the neutrino mass. Finally, physical and chemical properties of the decaying nuclides as well as their availability might become a show stopper for experiments based on these nuclides (as happened to the experiments with rhenium). Thus, it is of interest to search for other beta transitions that have an optimum set of “suitability” criteria and hence along with the  $\beta^-$  decay of tritium and the EC in  $^{163}\text{Ho}$  might be employed for the determination of the neutrino mass.

PTMS focuses on one of these criteria—the smallness of the  $Q$  value. It follows two different ways: the search for beta transitions with small decay energies (1) between the nuclear ground states and (2) between the nuclear ground state of the parent nuclide and a nuclear excited state of the daughter nuclide.

Of particular interest are electron-capture transitions due to the fact that their probability is defined by the difference  $Q_\nu \equiv Q - B_i$ , where  $B_i$  is the binding energy of the electron captured from the  $i$ -orbital. This difference could be very small for one of electron orbitals in the atom, which would result in a very small neutrino energy and hence in a high sensitivity of this electron-capture channel to the neutrino mass. Thus, measurements with low uncertainty of the  $Q$  values of potentially interesting EC-transitions shed light on the size of  $Q_\nu$ .

Two such ground-to-ground-state EC transitions,  $^{194}\text{Hg} \rightarrow ^{194}\text{Au}$  [23] and  $^{202}\text{Pb} \rightarrow ^{202}\text{Tl}$  [68], already have been addressed at the ISOLTRAP facility at CERN using the ToF-ICR technique.

The obtained  $Q$  value of 29(4) keV of the EC in  $^{194}\text{Hg}$  substantially deviates from that of 69(14) keV given in the Atomic Mass Evaluation (AME) table before these measurements and, although the K-electron capture is forbidden, suggests a possible determination of the neutrino mass by a microcalorimetric measurement of the de-excitation spectrum from L-capture in  $^{194}\text{Hg}$ . The total energy of the electron neutrino in this case is  $Q_\nu = 15(4)$  keV.

The  $Q$  value of the EC in  $^{202}\text{Pb}$  determined with ISOLTRAP is 38.8(43) keV. The lowest positive  $Q_\nu$  is for the L-capture and is equal to 23.5(43) keV. If only the magnitude of the  $Q$  value is considered, then one can conclude that neither the EC in  $^{194}\text{Hg}$  nor the EC in  $^{202}\text{Pb}$  can compete in terms of sensitivity to the neutrino mass with the EC in  $^{163}\text{Ho}$ .

Although ground-to-ground-state beta transitions are the primary choice for experiments on the determination of the neutrino mass due to several reasons, the number of such beta transitions that are potentially suitable for a precise neutrino-mass determination is in fact limited (see Fig. 1 in [23]). More chances to find a beta transition with a very small energy of

**Table 2** The most promising beta transitions from the ground state to excited states with ultra-low decay energies [40]

Decay	Allowed	First-forbidden
$\beta^-$	$^{131}\text{I}$ , $^{136}\text{Cs}$ , $^{188}\text{W}$	$^{154-156}\text{Eu}$ , $^{183}\text{Ta}$
EC	$^{57}\text{Ni}$ , $^{77}\text{Br}$ , $^{175}\text{Hf}$ , $^{200}\text{Tl}$	$^{75}\text{Se}$ , $^{156,157}\text{Tb}$ , $^{173}\text{Lu}$ , $^{190}\text{Ir}$
$\beta^+$	$^{79}\text{Kr}$	$^{146}\text{Eu}$

the emitted neutrino can be found among ground-to-excited-state beta transitions simply due to their large number [40]. The main criterion of choice here is the proximity of the mass difference between the ground states of the parent and daughter nuclides to the energy of the excited state populated in the beta process. The allowed and first-forbidden transitions from [40] are given in Table 2.

The mass differences between the ground states of the parent and daughter nuclides of some of the beta transitions with decay energies smaller than 1 keV already have been determined with Penning traps with a sub-keV/c<sup>2</sup> uncertainty (Table 3). It should be noted nevertheless that the ultra-low decay values alone of these beta transitions do not guarantee a high sensitivity to the determination of the neutrino mass. This is due to a combination of ultra-low decay energy and often a high degree of forbiddenness of these transitions, which leads to a very small total probability of the transition to an excited state in comparison to that to the ground state.

### Mass-difference measurements for the search for keV sterile neutrinos and relic neutrinos

There are no conceptual restrictions for a very broad mass range of sterile neutrinos. PTMS can contribute to the search for sterile neutrinos with keV/c<sup>2</sup> masses that can be attributed to Warm Dark Matter (WDM) [6]. The neutrino electron flavor state can be considered a mixture of the active and sterile neutrino mass eigenstates with the corresponding unitary mixing matrix. Since all the masses of active neutrinos are much smaller than the mass of the sterile one, we can consider on the keV/c<sup>2</sup> scale a simplified version of a mixing of one active mass eigenstate with  $m_i \ll 1 \text{ eV}/c^2$  and one sterile neutrino mass eigenstate with  $m_s$  on the keV/c<sup>2</sup> scale.

In a  $\beta^-$  decay energy spectrum of emitted electron the sterile neutrino reveals itself as a kink located at an energy which is a difference between the  $Q$  value of  $\beta^-$  decay and the keV/c<sup>2</sup> sterile neutrino mass value.

In electron-capture processes one can search for hints of the existence of the sterile neutrino in two ways. The first method is similar to that employed in  $\beta^-$  decay processes. One searches in the atomic de-excitation spectrum of the EC for a kink at an energy which is a difference between the  $Q$  value of the EC and the keV/c<sup>2</sup> sterile neutrino mass value.

**Table 3** The smallest ( $\leq 1$  keV) decay energy values between the mother ground state and daughter excited states of nuclides

Parent nuclide	Half-life	Daughter nuclide	Populated excited state in The daughter nuclide/keV	Decay energy / keV	References
$^{75}\text{Se}$	119.8 d	$^{75}\text{As}$	865.4(5)	0.64(51)	[53]
$^{115}\text{In}$	$4 \cdot 10^{14}$ y	$^{115}\text{Cd}$	497.334(22)	0.35(17)	[69]
				0.155(24)	[47]
				0.147(10)	[72]
$^{135}\text{Cs}$	$2.3 \cdot 10^6$ y	$^{135}\text{Ba}$	268.218(20)	0.44(31)	[18]
$^{155}\text{Tb}$	5.32 d	$^{155}\text{Gd}$	815.731(3)	-0.79(18)	[37]
$^{159}\text{Dy}$	144.4 d	$^{159}\text{Tb}$	363.5449	1.18(19)	[36]

The second method is based on the comparison of the probabilities to capture an electron from different atomic orbitals [30]. The probability  $\lambda_i$  to capture an electron by a nucleus from the  $i$  atomic orbital depends on the mass of the sterile neutrino. The ratios of the experimental probabilities  $\lambda_i/\lambda_j$  from atomic orbitals  $i$  and  $j$  can be determined from the areas under the peaks in the atomic de-excitation spectrum, whereas the theoretical ratios (i.e. without the sterile neutrino contribution) can be precisely calculated taking into account the cancellation of the nuclear matrix elements in the probability ratios. The electron wave functions can be calculated only with a certain non-vanishing uncertainty. In order to exclude this origin of uncertainty the same ratios for the probabilities in different isotopes of the same chemical element must be compared. In this case the influence of the electron wave functions is cancelled to large extend and the sensitivity to the amplitude of the sterile neutrino mass eigenstate can be considerably increased. The sensitivity to the amplitude of the sterile neutrino mass eigenstate depends on an accurate determination of atomic mass differences of studied isotopes. In [30] a list of promising EC transitions, e.g. EC in  $^{157}\text{Tb}$ ,  $^{163}\text{Ho}$ ,  $^{179}\text{Ta}$ ,  $^{193}\text{Pt}$ ,  $^{202}\text{Pb}$ ,  $^{205}\text{Pb}$  and  $^{235}\text{Np}$ , for a search for the sterile neutrino is given which masses have to be determined with high precision.

Relic neutrinos are regular neutrinos formed as a result of the Big Bang. Due to their extremely small interaction cross-section with matter they still roam around us forming a cosmic relic neutrino background. Their study can yield valuable information on an early history of the Universe. Although a direct observation of the cosmic neutrino background causes a great difficulty because relic neutrinos have very low energy, on average  $E_\nu = 0.00055$  eV, and an average density of just  $56 \text{ cm}^{-3}$ , nevertheless, a direct detection of relic neutrinos in experiments is the only way to confirm their existence.

One of proposed direct methods for an observation of relic neutrinos is their capture on nuclei that undergo  $\beta^-$  decay [14]. First attempts to observe relic neutrinos have been already undertaken in the KATRIN experiment util-

ising tritium [2]. Another proposed method for an observation of relic antineutrinos is their resonant absorption by nuclides that undergo nuclear electron capture [67]. The resonant absorption implies that the sum of the decay energy  $Q_{EC}$  and antineutrino mass  $m_\nu$  is slightly larger than the sum of nuclear excitation  $E^*$  and electron binding energy  $B_i$  of the electron captured from the  $i$ -orbital:

$$Q_{EC} + m_\nu c^2 \geq E^* + B_i. \quad (9)$$

Thus, the role of PTMS is a search for electron-capture transitions whose  $Q_{EC}$  values allow for a resonant capture of relic antineutrinos. There is a bunch of EC-decaying nuclides the  $Q_{EC}$  values of which are not known precisely enough, e.g.  $^{157}\text{Tb}$  [67],  $^{131}\text{Ba}$ ,  $^{159}\text{Dy}$ ,  $^{175}\text{Hf}$ ,  $^{195}\text{Au}$  and  $^{243}\text{Cm}$  [45], some of which might become suitable for the detection of relic antineutrinos.

### Mass-difference measurements for experiments for the search for neutrinoless double electron capture

It is still not known whether neutrinos are Dirac or Majorana particles. The most convenient and maybe at present the only way to unambiguously clarify the nature of the neutrino-antineutrino duality consists in the observation of the neutrinoless double-beta processes: (1) double electron emission ( $2\beta^-$  decay), (2) double positron emission, (3) one-electron capture with one-positron emission, or (4) double electron capture (2EC). These processes are only possible if neutrinos and antineutrinos are identical particles, i.e. Majorana particles, and the conservation of the total lepton number is violated. Since these processes are not allowed in the Standard Model, their observation will thus manifest new physics beyond the Standard Model.

In this section the contribution of PTMS to experiments on the search for neutrinoless double electron capture is briefly reviewed. In general neutrinoless 2EC is expected to have smaller transition probability than neutrinoless  $2\beta^-$  decay. But in some cases the probability of neutrinoless 2EC can

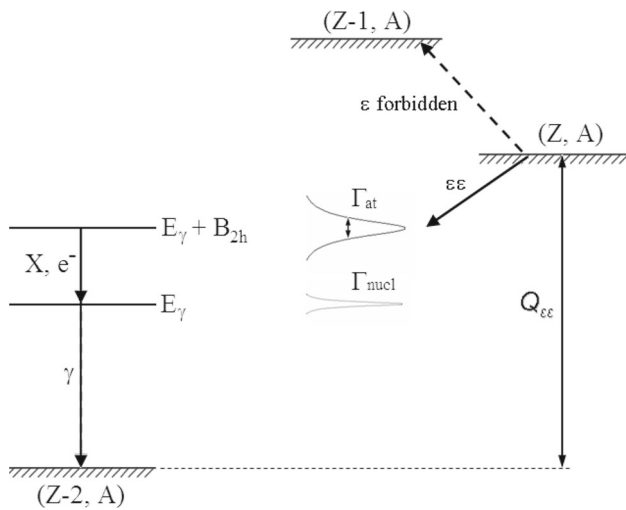


**Fig. 6** An energy diagram of double-electron capture between two neutral atoms with the same mass number  $A$ . The intermediate nuclide  $(Z-1, A)$  energetically cannot be populated. Both the atomic level de-excitation (by X-rays or electrons) and the nuclear de-excitation by gamma-rays are shown.  $\Gamma_{at}$  and  $\Gamma_{nucl}$  are the atomic and nuclear level widths ( $\Gamma_{at} \gg \Gamma_{nucl}$ )

be resonantly enhanced by many orders of magnitude and hence becomes comparable to that of neutrinoless  $2\beta^-$  decay. The transition probability of neutrinoless 2EC is resonantly enhanced if the initial and final states of the atom are degenerate in energy. In the transition probability a so-called resonance enhancement coefficient  $r_{\epsilon\epsilon}$  appears, which is defined as ([8])

$$r_{\epsilon\epsilon} = \frac{\Gamma_{2h}}{\Delta^2 + \Gamma_{2h}^2/4}. \quad (10)$$

Here,  $\Gamma_{2h}$  is the sum of the decay widths of the excited daughter atom, and  $\Delta$  is the degeneracy parameter given by

$$\Delta = Q_{\epsilon\epsilon} - B_{2h} - E_{\gamma}, \quad (11)$$

where  $Q_{\epsilon\epsilon}$  is the total decay energy,  $B_{2h}$  is the binding energy of the double-electron hole in the atomic shell of the daughter atom, and  $E_{\gamma}$  is the excitation energy of the daughter nucleus.

As can be seen the enhancement coefficient  $r_{\epsilon\epsilon}$  will be maximal when the degeneracy parameter  $\Delta$  is close to zero. Although the phenomenon of the resonant enhancement was predicted some decades ago, the search for resonantly enhanced neutrinoless double-electron capture transitions for a long time was hampered by the lack of precise experimental values of  $Q_{\epsilon\epsilon}$ , which accuracy was larger than keV, whereas the values of  $B_{2h}$  and  $E_{\gamma}$  are usually known with much better accuracy. To reach a similar level of precision for  $Q_{\epsilon\epsilon}$  the PTMS has to be employed. A general decay scheme of neutrinoless 2EC is shown in Fig. 6.

The most favourable cases are neutrinoless 2EC transitions between  $0^+$  nuclear ground states that proceed via a capture of two s-electrons from K-shell. For such transitions the neutrinoless mode dominates since the two-neutrino mode is strongly suppressed by phase space. With the Penning-trap mass spectrometer SHIPTRAP the  $Q_{\epsilon\epsilon}$  values of three such 2EC transitions, namely  $^{152}\text{Gd} \rightarrow ^{152}\text{Sm}$ ,  $^{164}\text{Er} \rightarrow ^{164}\text{Dy}$  and  $^{180}\text{W} \rightarrow ^{180}\text{Hf}$ , were determined with a few 100 eV uncertainty ([8]). The measurement yielded that the degeneracy parameter  $\Delta$  of neither of these transitions is small enough to consider some of these transitions fully resonantly enhanced. Among these three transitions  $^{152}\text{Gd} \rightarrow ^{152}\text{Sm}$  has the smallest degeneracy parameter  $\Delta$  of 0.83(18) keV and an expected half-life larger than  $10^{28}$  years.

Although neutrinoless 2EC transitions between  $0^+$  nuclear ground states are preferable for the search for neutrinoless double-beta processes, neutrinoless 2EC transitions between the mother nuclear ground state and a daughter nuclear excited state are of interest too. The  $Q_{\epsilon\epsilon}$  values of more than a dozen such transitions were determined with various, predominantly online high-precision Penning-trap mass spectrometers ([8]). This measurement campaign revealed that the  $^{156}\text{Dy} \rightarrow ^{156}\text{Gd}$  transition to the nuclear excited state with an excitation energy of 1988.5(2) keV is fully resonantly enhanced with a degeneracy factor  $\Delta$  of 0.04(10) keV. Unfortunately, the process proceeds via a capture of two p-electrons from L-shell. For such transitions the nuclear matrix elements are small and thus the half-lives are too long in order to consider them suitable for the search for neutrinoless double-beta processes.

## Conclusion and Outlook

A rapid development of Penning-trap mass spectrometry over the past two decades has made this technique of great importance for many studies carried out at the frontiers of fundamental physics, in particular for neutrino physics. A good example of such a development is the Penning-trap mass spectrometer PENTATRAP at the Max-Planck Institute for Nuclear Physics. The implementation of such unique features as simultaneous cyclotron-frequency measurements in several Penning traps on highly charged ions of different nuclides of interest allows for mass-ratio measurements on a broad range of long-lived nuclides with fractional uncertainties down to few parts in  $10^{12}$ . This paves the path to measurements on a level of an eV of the  $Q$  values of various beta processes that are relevant to the determination of the (anti)neutrino mass, the search for sterile and relic neutrinos.

Also Penning-trap mass spectrometers that are usually devoted to mass measurements on short-lived nuclides with uncertainties down to about  $10^{-9}$  have significantly contributed to studies of neutrinoless double-beta processes.

These studies aim to shed light on one of the open problems of neutrino physics—are neutrinos Dirac or Majorana particles? Is the total lepton number conserved?

In general, the modern state of Penning-trap mass spectrometry opens the doors to mass-ratio measurements relevant to many fundamental studies that go beyond the scope of this paper. Just to mention a few: PTMS can be of great assistance in the search for dark matter and the fifth force, low-lying atomic metastable states suitable for a new generation of ion clocks and can contribute to the determination of the  $\alpha$  constant. This list is by far not exhaustive and will steadily expand as the development of PTMS is going on.

**Acknowledgements** The authors thank Klaus Blaum, the members of the PENTATRAP group and the ECHo collaboration for productive discussions.

**Funding Information** Open Access funding enabled and organized by Projekt DEAL.

**Data Availability** This manuscript has no associated data or the data will not be deposited. [Authors' comment: The manuscript does not present the so-far unpublished results of a particular experiment. It is an overview of the contribution of many Penning-trap experiments to neutrino physics. All these experiments and their results are properly cited. Please look up the cited papers for the associated data.]

**Open Access** This article is licensed under a Creative Commons Attribution 4.0 International License, which permits use, sharing, adaptation, distribution and reproduction in any medium or format, as long as you give appropriate credit to the original author(s) and the source, provide a link to the Creative Commons licence, and indicate if changes were made. The images or other third party material in this article are included in the article's Creative Commons licence, unless indicated otherwise in a credit line to the material. If material is not included in the article's Creative Commons licence and your intended use is not permitted by statutory regulation or exceeds the permitted use, you will need to obtain permission directly from the copyright holder. To view a copy of this licence, visit <http://creativecommons.org/licenses/by/4.0/>.

## References

1. M. Aker, A. Beglarian, J. Behrens, A. Berlev, U. Besserer, B. Bieringer, F. Block, S. Bobien, M. Böttcher, B. Bornschein, L. Bornschein, T. Brunst, T.S. Caldwell, R.M.D. Carney, L. La Cascio, S. Chilingaryan, W. Choi, K. Debowski, M. Deffert, M. Descher, D. Diaz Barrero, P.J. Doe, O. Dragoun, G. Drexlin, K. Eitel, E. Ellinger, R. Engel, S. Enomoto, A. Felden, J.A. Formaggio, F.M. Fränkle, G.B. Franklin, F. Friedel, A. Fulst, K. Gauda, A.S. Gavin, W. Gil, F. Glück, R. Grössle, R. Gumsheimer, V. Hannen, N. Haußmann, K. Helbing, S. Hickford, R. Hiller, D. Hillesheimer, D. Hinz, T. Höhn, T. Houdy, A. Huber, A. Jansen, C. Karl, F. Kellerer, J. Kellerer, M. Kleifges, M. Klein, C. Köhler, L. Köllenberger, A. Kopmann, M. Korzeczek, A. Kovalík, B. Krasch, H. Krause, L. La Cascio, T. Lasserre, T.L. Le, O. Lebeda, B. Lehnert, A. Lokhov, M. Machatschek, E. Malcherek, M. Mark, A. Marsteller, E.L. Martin, C. Melzer, S. Mertens, J. Mostafa, K. Müller, H. Neumann, S. Niemes, P. Oelpmann, D.S. Parno, A.W.P. Poon, J.M.L. Poyato, F. Priester, J. Ráliš, S. Ramachandran, R.G.H. Robertson, W. Rodejohann, C. Rodenbeck, M. Röllig, C. Rötteler, M. Ryšavý, R. Sack, A. Saenz, R. Salomon, P. Schäfer, L. Schimpf, M. Schlösser, K. Schlösser, L. Schlüter, S. Schneidewind, M. Schrank, A. Schwemmer, M. Šefčík, V. Sibille, D. Siegmann, M. Slezák, F. Spanier, M. Steidl, M. Sturm, M. Sun, D. Tcherniakhovski, H.H. Telle, L.A. Thorne, T. Thümmler, N. Titov, I. Tkachev, K. Urban, K. Valerius, D. Vénos, A.P. Vizcaya Hernández, C. Weinheimer, S. Welte, J. Wendel, J.F. Wilkerson, J. Wolf, S. Wüstling, J. Wydra, W. Xu, Y.-R. Yen, S. Zadorogny, G. Zeller, T.K. Collaboration *Nature Physics* **18**(2), 160–166 (2022a)
2. M. Aker, D. Batzler, A. Beglarian, J. Behrens, A. Berlev, U. Besserer, B. Bieringer, F. Block, S. Bobien, B. Bornschein, L. Bornschein, M. Böttcher, T. Brunst, T.S. Caldwell, R.M.D. Carney, S. Chilingaryan, W. Choi, K. Debowski, M. Descher, D. Diaz Barrero, P.J. Doe, O. Dragoun, G. Drexlin, F. Edzards, K. Eitel, E. Ellinger, R. Engel, S. Enomoto, A. Felden, J.A. Formaggio, F.M. Fränkle, G.B. Franklin, F. Friedel, A. Fulst, K. Gauda, A.S. Gavin, W. Gil, F. Glück, R. Grössle, R. Gumsheimer, V. Hannen, N. Haußmann, K. Helbing, S. Hickford, R. Hiller, D. Hillesheimer, D. Hinz, T. Höhn, T. Houdy, A. Huber, A. Jansen, C. Karl, F. Kellerer, J. Kellerer, M. Kleifges, M. Klein, C. Köhler, L. Köllenberger, A. Kopmann, M. Korzeczek, A. Kovalík, B. Krasch, H. Krause, L. La Cascio, T. Lasserre, T.L. Le, O. Lebeda, B. Lehnert, A. Lokhov, M. Machatschek, E. Malcherek, M. Mark, A. Marsteller, E.L. Martin, C. Melzer, S. Mertens, J. Mostafa, K. Müller, H. Neumann, S. Niemes, P. Oelpmann, D.S. Parno, A.W.P. Poon, J.M.L. Poyato, F. Priester, J. Ráliš, S. Ramachandran, R.G.H. Robertson, W. Rodejohann, C. Rodenbeck, M. Röllig, C. Rötteler, M. Ryšavý, R. Sack, A. Saenz, R. Salomon, P. Schäfer, L. Schimpf, M. Schlösser, K. Schlösser, L. Schlüter, S. Schneidewind, M. Schrank, A. Schwemmer, M. Šefčík, V. Sibille, D. Siegmann, M. Slezák, F. Spanier, M. Steidl, M. Sturm, H.H. Telle, L.A. Thorne, T. Thümmler, N. Titov, I. Tkachev, K. Urban, K. Valerius, D. Vénos, A.P. Vizcaya Hernández, C. Weinheimer, S. Welte, J. Wendel, C. Wiesinger, J.F. Wilkerson, J. Wolf, S. Wüstling, J. Wydra, W. Xu, S. Zadorogny, G. Zeller, New constraint on the local relic neutrino background overdensity with the first katrin data runs. *Phys. Rev. Lett.* **129**, 011806 (2022b)
3. A. Alessandrello, J.W. Beerman, C. Brofferio, O. Cremonesi, E. Fiorini, A. Giuliani, E.E. Haller, B. Margesin, A. Monfardini, A. Nucciotti, M. Pavan, G. Pessina, G. Pignateli, E. Previtali, L. Zanotti, M. Zen, Bolometric measurements of beta decay spectra of  $^{187}\text{Re}$  with crystals of silver perrhenate. *Phys. Lett. B* **457**(1), 253–260 (1999)
4. C. Arnaboldi, C. Brofferio, O. Cremonesi, E. Fiorini, C. Lo Bianco, L. Martensson, A. Nucciotti, M. Pavan, G. Pessina, S. Pirro, E. Previtali, M. Sisti, A. Giuliani, B. Margesin, M. Zen, Bolometric bounds on the antineutrino mass. *Phys. Rev. Lett.* **91**, 161802 (2003)
5. M.S. Athar, S.W. Barwick, T. Brunner, J. Cao, M. Danilov, K. Inoue, T. Kajita, M. Kowalski, M. Lindner, K.R. Long, N. Palanque-Delabrouille, W. Rodejohann, H. Schellman, K. Scholberg, S.-H. Seo, N.J.T. Smith, W. Winter, G.P. Zeller, R.Z. Funchal, Status and perspectives of neutrino physics. *Prog. Part. Nucl. Phys.* **124**, 103947 (2022)
6. F. Bezrukov, M. Shaposhnikov, Searching for dark matter sterile neutrinos in the laboratory. *Phys. Rev. D* **75**, 053005 (2007)
7. K. Blaum, Y.N. Novikov, G. Werth, Penning traps as a versatile tool for precise experiments in fundamental physics. *Contemp. Phys.* **51**(2), 149–175 (2010)
8. K. Blaum, S. Eliseev, F.A. Danevich, V.I. Tretyak, S. Kovalenko, M.I. Krivoruchenko, Y.N. Novikov, J. Suhonen, Neutrinoless double-electron capture. *Rev. Mod. Phys.* **92**, 045007 (2020)
9. K. Blaum, High-accuracy mass spectrometry with stored ions. *Phys. Rep.* **425**(1), 1–78 (2006)
10. M. Block, D. Ackermann, D. Beck, K. Blaum, M. Breitenfeldt, A. Chauduri, A. Doemer, S. Eliseev, D. Habs, S. Heinz, F. Herfurth, F.P. Hessberger, S. Hofmann, H. Geissel, H.-J. Kluge, V. Kolhinen,

G. Marx, J.B. Neumayr, M. Mukherjee, M. Petrick, W. Plass, W. Quint, S. Rahaman, C. Rauth, D. Rodríguez, C. Scheidenberger, L. Schweikhard, M. Suhonen, P.G. Thirolf, Z. Wang, C. Weber, the SHIPTRAP Collaboration, The ion-trap facility shiptrap. *Eur. Phys. J. A Hadrons and Nuclei* **25**(1), 49–50 (2005)

11. L.S. Brown, G. Gabrielse, Precision spectroscopy of a charged particle in an imperfect Penning trap. *Phys. Rev. A* **25**, 2423–2425 (1982)
12. L.S. Brown, G. Gabrielse, Geonium theory: Physics of a single electron or ion in a penning trap. *Rev. Mod. Phys.* **58**, 233–311 (1986)
13. C. Böhm, S. Sturm, A. Rischka, A. Dörr, S. Eliseev, M. Goncharov, M. Höcker, J. Ketter, F. Köhler, D. Marschall, J. Martin, D. Obieglo, J. Repp, C. Roux, R.X. Schüssler, M. Steigleder, S. Streubel, T. Wagner, J. Westermann, V. Wieder, R. Zirpel, J. Melcher, K. Blaum, An ultra-stable voltage source for precision penning-trap experiments. *Nucl. Instrum. Methods Phys. Res., Sect. A* **828**, 125–131 (2016)
14. A.G. Cocco, G. Mangano, M. Messina, Probing low energy neutrino backgrounds with neutrino capture on beta decaying nuclei. *J. Phys. Conf. Ser.* **110**(8), 082014 (2008)
15. E.A. Cornell, R.M. Weisskoff, K.R. Boyce, R.W. Flanagan, G.P. Lafyatis, D.E. Pritchard, Single-ion cyclotron resonance measurement of  $M(CO^+)/M(N_2^+)$ . *Phys. Rev. Lett.* **63**, 1674–1677 (1989)
16. E.A. Cornell, R.M. Weisskoff, K.R. Boyce, D.E. Pritchard, Mode coupling in a penning trap:  $\pi$  pulses and a classical avoided crossing. *Phys. Rev. A* **41**, 312–315 (1990)
17. E. Cosulich, G. Gallinaro, F. Gatti, S. Vitale, Detection of  $^{187}\text{Re}$  beta decay with a cryogenic microcalorimeter. preliminary results. *Phys. Lett. B* **295**(1), 143–147 (1992)
18. A. de Roubin, J. Kostensalo, T. Eronen, L. Canete, R.P. de Groote, A. Jokinen, A. Kankainen, D.A. Nesterenko, I.D. Moore, S. Rinta-Antila, J. Suhonen, M. Vilén, High-precision  $Q$ -value measurement confirms the potential of  $^{135}\text{Cs}$  for absolute antineutrino mass scale determination. *Phys. Rev. Lett.* **124**, 222503 (2020)
19. J. Dilling, D. Ackermann, J. Bernard, F.P. Hessberger, S. Hofmann, W. Hornung, H.J. Kluge, E. Lamour, M. Maier, R. Mann, G. Marx, R.B. Moore, G. Münzenberg, W. Quint, D. Rodriguez, M. Schädel, J. Schönfelder, G. Sikler, C. Toader, L. Vermeeren, C. Weber, G. Bollen, O. Engels, D. Habs, P. Thirolf, H. Backe, A. Dretzke, W. Lauth, W. Ludolfs, M. Sewitz, The shiptrap project: A capture and storage facility at GSI for heavy radionuclides from SHIP. *Hyperfine Interact.* **127**(1), 491–496 (2000)
20. J. Dilling, P. Bricault, M. Smith, H.-J. Kluge, The proposed TITAN facility at ISAC for very precise mass measurements on highly charged short-lived isotopes. *Nuclear Instruments and Methods in Physics Research Section B: Beam Interactions with Materials and Atoms* **204**, 492–496 (2003). 14th International Conference on Electromagnetic Isotope Separators and Techniques Related to their Applications
21. S. Eliseev, T. Eronen, Y.N. Novikov, Penning-trap mass spectrometry for neutrino physics. *International Journal of Mass Spectrometry* **349–350**, 102–106 (2013). 100 years of Mass Spectrometry
22. S.A. Eliseev, Y.N. Novikov, K. Blaum, Search for resonant enhancement of neutrinoless double-electron capture by high-precision penning-trap mass spectrometry. *J. Phys. G: Nucl. Part. Phys.* **39**(12), 124003 (2012)
23. S. Eliseev, C. Böhm, D. Beck, K. Blaum, M. Breitenfeldt, V.N. Fedossev, S. George, F. Herfurth, A. Herlert, H.-J. Kluge, M. Kowalska, D. Lunney, S. Naimi, D. Neidherr, Y.N. Novikov, M. Rosenbusch, L. Schweikhard, S. Schwarz, M. Seliverstov, K. Zuber, Direct mass measurements of  $^{194}\text{Hg}$  and  $^{194}\text{Au}$ : A new route to the neutrino mass determination? *Phys. Lett. B* **693**(4), 426–429 (2010)
24. S. Eliseev, K. Blaum, M. Block, C. Droese, M. Goncharov, E. Minaya Ramirez, D.A. Nesterenko, Y.N. Novikov, L. Schweikhard, Phase-imaging ion-cyclotron-resonance measurements for short-lived nuclides. *Phys. Rev. Lett.* **110**, 082501 (2013)
25. S. Eliseev, K. Blaum, M. Block, A. Dörr, C. Droese, T. Eronen, M. Goncharov, M. Höcker, J. Ketter, E.M. Ramirez, D.A. Nesterenko, Y.N. Novikov, L. Schweikhard, A phase-imaging technique for cyclotron-frequency measurements. *Appl. Phys. B* **114**(1), 107–128 (2014)
26. S. Eliseev, K. Blaum, M. Block, S. Chenmarev, H. Dorrer, C.E. Düllmann, C. Enss, P.E. Filianin, L. Gastaldo, M. Goncharov, U. Köster, F. Lautenschläger, Y.N. Novikov, A. Rischka, R.X. Schüssler, L. Schweikhard, A. Türler, Direct measurement of the mass difference of  $^{163}\text{Ho}$  and  $^{163}\text{Dy}$  Solves the  $Q$ -Value Puzzle for the Neutrino Mass Determination. *Phys. Rev. Lett.* **115**, 062501 (2015)
27. S. Eliseev, Y.N. Novikov, K. Blaum, Penning-trap mass spectrometry and neutrino physics. *Ann. Phys.* **525**(8–9), 707–719 (2013)
28. T. Eronen, V.S. Kolhinen, V.-V. Elomaa, D. Gorelov, U. Hager, J. Hakala, A. Jokinen, A. Kankainen, P. Karvonen, S. Kopecky, I.D. Moore, H. Penttilä, S. Rahaman, S. Rinta-Antila, J. Rissanen, A. Saastamoinen, J. Szczepo, C. Weber, J. Äystö, JYFLTRAP: a penning trap for precision mass spectroscopy and isobaric purification. *Eur. Phys. J. A* **48**(4), 46 (2012)
29. A.A. Esfahani, D.M. Asner, S. Böser, R. Cervantes, C. Claessens, L. de Viveiros, P.J. Doe, S. Doebleman, J.L. Fernandes, M. Fertl, E.C. Finn, J.A. Formaggio, D. Furse, M. Guigue, K.M. Heeger, A.M. Jones, K. Kazkaz, J.A. Kofron, C. Lamb, B.H. LaRoque, E. Machado, E.L. McBride, M.L. Miller, B. Monreal, P. Mohanmurthy, J.A. Nikkel, N.S. Oblath, W.C. Pettus, R.G.H. Robertson, L.J. Rosenberg, G. Rybka, D. Rysewyk, L. Saldaña, P.L. Slocum, M.G. Sternberg, J.R. Tedeschi, T. Thümmler, B.A. VanDevender, L.E. Vertatschitsch, M. Wachtendonk, J. Weintraub, N.L. Woods, A. Young, E.M. Zayas, Determining the neutrino mass with cyclotron radiation emission spectroscopy Project 8. *J. Phys. G: Nucl. Part. Phys.* **44**(5), 054004 (2017)
30. P.E. Filianin, K. Blaum, S.A. Eliseev, L. Gastaldo, Y.N. Novikov, V.M. Shabaev, I.I. Tupitsyn, J. Vergados, On the keV sterile neutrino search in electron capture. *J. Phys. G: Nucl. Part. Phys.* **41**(9), 095004 (2014)
31. P. Filianin, C. Lyu, M. Door, K. Blaum, W.J. Huang, M. Haverkort, P. Indelicato, C.H. Keitel, K. Kromer, D. Lange, Y.N. Novikov, A. Rischka, R.X. Schüssler, C. Schweiger, S. Sturm, S. Ulmer, Z. Harman, S. Eliseev, Direct  $Q$ -value determination of the  $\beta^-$  Decay of  $^{187}\text{Re}$ . *Phys. Rev. Lett.* **127**, 072502 (2021)
32. J.A. Formaggio, A.L.C. de Gouvêa, R.G.H. Robertson, Direct measurements of neutrino mass. *Physics Reports* **914**, 1–54 (2021). Direct measurements of neutrino mass
33. G. Gabrielse, The true cyclotron frequency for particles and ions in a Penning trap. *Int. J. Mass Spectrom.* **279**(2), 107–112 (2009)
34. M. Galeazzi, F. Fontanelli, F. Gatti, S. Vitale, End-point energy and half-life of the  $^{187}\text{Re}$   $\beta$  decay. *Phys. Rev. C* **63**, 014302 (2000)
35. L. Gastaldo, K. Blaum, K. Chrysalidis, T. Day Goodacre, A. Domula, M. Door, H. Dorrer, C.E. Düllmann, K. Eberhardt, S. Eliseev, C. Enss, A. Faessler, P. Filianin, A. Fleischmann, D. Fonnesu, L. Gamer, R. Haas, C. Hassel, D. Hengstler, J. Jochum, K. Johnston, U. Kebischull, S. Kempf, T. Kieck, U. Küster, S. Lahiri, M. Maiti, F. Mantegazzini, B. Marsh, P. Neroutsos, Y.N. Novikov, P.C.O. Ranitzsch, S. Rothe, A. Rischka, A. Saenz, O. Sander, F. Schneider, S. Scholl, R.X. Schüssler, C. Schweiger, F. Simkovic, T. Stora, Z. Szűcs, A. Türler, M. Veinhard, M. Weber, M. Wegner, K. Wendt, K. Zuber, The electron capture in  $^{163}\text{Ho}$  experiment ECHo. *Eur. Phys. J. Spec. Top.* **226**(8), 1623–1694 (2017)
36. Z. Ge, T. Eronen, K.S. Tyrin, J. Kotila, J. Kostensalo, D.A. Nesterenko, O. Beliuskina, R. de Groote, A. de Roubin, S. Geldhof, W. Gins, M. Hukkanen, A. Jokinen, A. Kankainen, Á. Koszorús, M.I. Krivoruchenko, S. Kujanpää, I.D. Moore, A. Raggio, S. Rinta-Antila, J. Suhonen, V. Virtanen, A.P. Weaver, A. Zadvornaya,  $^{159}\text{dy}$

electron-capture: A new candidate for neutrino mass determination. *Phys. Rev. Lett.* **127**, 272301 (2021)

37. Z. Ge, T. Eronen, A. de Roubin, J. Kostensalo, J. Suhonen, D.A. Nesterenko, O. Beliuskina, R. de Groote, C. Delafosse, S. Geldhof, W. Gins, M. Hukkanen, A. Jokinen, A. Kankainen, J. Kotila, Á. Koszorús, I.D. Moore, A. Raggio, S. Rinta-Antila, V. Virtanen, A.P. Weaver, A. Zadvornaya. *Phys. Rev. C* **106**(1) (2022)

38. G. Gräff, H. Kalinowsky, J. Traut, A direct determination of the proton electron mass ratio. *Zeitschrift für Physik A Atoms Nucl.* **297**(1), 35–39 (1980)

39. F. Heiße, S. Rau, F. Köhler-Langes, W. Quint, G. Werth, S. Sturm, K. Blaum, High-precision mass spectrometer for light ions. *Phys. Rev. A* **100**, 022518 (2019)

40. D.K. Kebelbeck, R. Bhandari, N.D. Gamage, M.H. Gamage, M. Redshaw (2022). <https://doi.org/10.48550/ARXIV.2201.08790>

41. J. Ketelaer, J. Krämer, D. Beck, K. Blaum, M. Block, K. Eberhardt, G. Eitel, R. Ferrer, C. Geppert, S. George, F. Herfurth, J. Ketter, S. Nagy, D. Neidherr, R. Neugart, W. Nörtershäuser, J. Repp, C. Smorra, N. Trautmann, C. Weber, Triga-spec: A setup for mass spectrometry and laser spectroscopy at the research reactor triga mainz. *Nucl. Instrum. Methods Phys. Res., Sect. A* **594**(2), 162–177 (2008)

42. H.-J. Kluge, G. Bollen, Isoltrap: A tandem Penning trap mass spectrometer for radioactive isotopes. *Hyperfine Interact.* **81**(1), 15–26 (1993)

43. M. Kretzschmar, The Ramsey method in high-precision mass spectrometry with Penning traps: Theoretical foundations. *Int. J. Mass Spectrom.* **264**(2), 122–145 (2007)

44. M. König, G. Bollen, H.-J. Kluge, T. Otto, J. Szerypo, Quadrupole excitation of stored ion motion at the true cyclotron frequency. *Int. J. Mass Spectrom. Ion Processes* **142**(1), 95–116 (1995)

45. J.-Y. Lee, Y. Kim, S. Chiba, (arXiv, 2018)

46. B. Monreal, J.A. Formaggio, Relativistic cyclotron radiation detection of tritium decay electrons as a new technique for measuring the neutrino mass. *Phys. Rev. D* **80**, 051301 (2009)

47. B.J. Mount, M. Redshaw, E.G. Myers,  $Q$  Value of  $^{115}\text{In} \rightarrow ^{115}\text{Sn}(3/2^+)$ : The Lowest Known Energy  $\beta$  Decay. *Phys. Rev. Lett.* **103**, 122502 (2009)

48. E.G. Myers, A. Wagner, H. Kracke, B.A. Wesson, Atomic masses of tritium and helium-3. *Phys. Rev. Lett.* **114**, 013003 (2015)

49. S. Nagy, T. Fritioff, M. Björkhage, I. Bergström, R. Schuch, *Europhys. Lett. (EPL)* **74**(3), 404–410 (2006)

50. D.A. Nesterenko, S. Eliseev, K. Blaum, M. Block, S. Chenmarev, A. Dörr, C. Droese, P.E. Filianin, M. Goncharov, E. Minaya Ramirez, Y.N. Novikov, L. Schweikhard, V.V. Simon, Direct determination of the atomic mass difference of  $^{187}\text{Re}$  and  $^{187}\text{Os}$  for neutrino physics and cosmochronology. *Phys. Rev. C* **90**, 042501 (2014)

51. Y.N. Novikov, T. Enqvist, A.N. Erykalov, F.v. Feilitzsch, J. Hissa, K. Loo, D.A. Nesterenko, L. Oberauer, F. Thorne, W. Trzaska, J.D. Vergados, M. Wurm, (arXiv, 2011). <https://doi.org/10.48550/ARXIV.1110.2983>

52. A. Nucciotti, B. Alpert, M. Balata, D. Becker, D. Bennett, A. Bevilacqua, M. Biasotti, V. Ceriale, G. Ceruti, D. Corsini, M. De Gerone, R. Dressler, M. Favazzani, E. Ferri, J. Fowler, G. Gallucci, J. Gard, F. Gatti, A. Giachero, J. Hays-Wehle, S. Heinitz, G. Hilton, U. Köster, M. Lusignoli, J. Mates, S. Nisi, A. Orlando, L. Parodi, G. Pessina, A. Puiu, S. Ragazzi, C. Reintsema, M. Ribeiro-Gomez, D. Schmidt, D. Schuman, F. Siccardi, D. Swetz, J. Ullom, L. Vale, Status of the holmes experiment to directly measure the neutrino mass. *J. Low Temp. Phys.* **193**(5), 1137–1145 (2018)

53. M. Ramalho, Z. Ge, T. Eronen, D.A. Nesterenko, J. Jaatinen, A. Jokinen, A. Kankainen, J. Kostensalo, J. Kotila, M.I. Krivoruchenko, J. Suhonen, K.S. Tyrin, V. Virtanen, *Physical Review C* **106**(1) (2022)

54. J. Repp, C. Böhm, J.R. Crespo López-Urrutia, A. Dörr, S. Eliseev, S. George, M. Goncharov, Y.N. Novikov, C. Roux, S. Sturm, S. Ulmer, K. Blaum, PENTATRAP: a novel cryogenic multi-Penning-trap experiment for high-precision mass measurements on highly charged ions. *Appl. Phys. B* **107**(4), 983–996 (2012)

55. R. Ringle, G. Bollen, A. Prinke, J. Savory, P. Schury, S. Schwarz, T. Sun, The LEBIT 9.4T Penning trap mass spectrometer. *Nuclear Instruments and Methods in Physics Research Section A: Accelerators, Spectrometers, Detectors and Associated Equipment* **604**(3), 536–547 (2009)

56. G. Savard, S. Becker, G. Bollen, H.-J. Kluge, R.B. Moore, T. Otto, L. Schweikhard, H. Stolzenberg, U. Wiess, A new cooling technique for heavy ions in a penning trap. *Phys. Lett. A* **158**(5), 247–252 (1991)

57. G. Savard, R.C. Barber, C. Boudreau, F. Buchinger, J. Caggiano, J. Clark, J.E. Crawford, H. Fukutani, S. Gulick, J.C. Hardy, A. Heinz, J.K.P. Lee, R.B. Moore, K.S. Sharma, J. Schwartz, D. Seweryniak, G.D. Sprouse, J. Vaz, The Canadian Penning Trap Spectrometer at Argonne, in *Atomic Physics at Accelerators: Mass Spectrometry* (Springer Netherlands, 2001), pp. 223–230

58. C. Schweiger, in preparation

59. C. Schweiger, C.M. König, J.R. Crespo López-Urrutia, M. Door, H. Dorrer, C.E. Düllmann, S. Eliseev, P. Filianin, W. Huang, K. Kromer, P. Micke, M. Müller, D. Renisch, A. Rischka, R.X. Schüssler, K. Blaum, Production of highly charged ions of rare species by laser-induced desorption inside an electron beam ion trap. *Rev. Sci. Instrum.* **90**(12), 123201 (2019)

60. R.X. Schüssler, H. Bekker, M. Brass, H. Cakir, J.R. Crespo López-Urrutia, M. Door, P. Filianin, Z. Harman, M.W. Haverkort, W.J. Huang, P. Indelicato, C.H. Keitel, C.M. König, K. Kromer, M. Müller, Y.N. Novikov, A. Rischka, C. Schweiger, S. Sturm, S. Ulmer, S. Eliseev, K. Blaum, Detection of metastable electronic states by Penning trap mass spectrometry. *Nature* **581**(7806), 42–46 (2020)

61. W. Shi, M. Redshaw, E.G. Myers, Atomic masses of  $^{32,33}\text{S}$ ,  $^{84,86}\text{Kr}$ , and  $^{129,132}\text{Xe}$  with uncertainties 01 ppb. *Phys. Rev. A* **72**, 022510 (2005)

62. C. Smorra, K. Blaum, L. Bojtar, M. Borchert, K.A. Franke, T. Higuchi, N. Leefer, H. Nagahama, Y. Matsuda, A. Mooser, M. Niemann, C. Ospelkaus, W. Quint, G. Schneider, S. Sellner, T. Tanaka, S. Van Gorp, J. Walz, Y. Yamazaki, S. Ulmer, Base—the baryon antibaryon symmetry experiment. *Eur. Phys. J. Spec. Top.* **224**(16), 3055–3108 (2015)

63. S. Sturm, A. Wagner, B. Schabinger, J. Zatorski, Z. Harman, W. Quint, G. Werth, C.H. Keitel, K. Blaum,  $g$  Factor of Hydrogenlike  $^{28}\text{Si}^{13+}$ . *Phys. Rev. Lett.* **107**, 023002 (2011)

64. R.S. Van Dyck, D.L. Farnham, P.B. Schwinberg, Tritium-helium-3 mass difference using the Penning trap mass spectroscopy. *Phys. Rev. Lett.* **70**, 2888–2891 (1993)

65. C. Velte, F. Ahrens, A. Barth, K. Blaum, M. Brass, M. Door, H. Dorrer, C.E. Düllmann, S. Eliseev, C. Enss, P. Filianin, A. Fleischmann, L. Gastaldo, A. Goeggemann, T.D. Goodacre, M.W. Haverkort, D. Hengstler, J. Jochum, K. Johnston, M. Keller, S. Kempf, T. Kieck, C.M. König, U. Köster, K. Kromer, F. Mantegazzini, B. Marsh, Y.N. Novikov, F. Piquemal, C. Riccio, D. Richter, A. Rischka, S. Rothe, R.X. Schüssler, C. Schweiger, T. Stora, M. Wegner, K. Wendt, M. Zampaolo, K. Zuber, High-resolution and low-background  $^{163}\text{Ho}$  spectrum: interpretation of the resonance tails. *Eur. Phys. J. C* **79**(12), 1026 (2019)

66. J.L. Verdi, S. Djekic, S. Stahl, T. Valenzuela, M. Vogel, G. Werth, H.-J. Kluge, W. Quint, Determination of the g-Factor of Single Hydrogen-Like Ions by Mode Coupling in a Penning Trap. *Phys. Scr.* **T112**(1), 68 (2004)

67. J.D. Vergados, Y.N. Novikov, Prospects of detection of relic antineutrinos by resonant absorption in electron capturing nuclei. *J. Phys. G: Nucl. Part. Phys.* **41**(12), 125001 (2014)

68. A. Welker, P. Filianin, N.A.S. Althubiti, D. Atanasov, K. Blaum, T.E. Cocolios, S. Eliseev, F. Herfurth, S. Kreim, D. Lunney, V.

Manea, D. Neidherr, Y. Novikov, M. Rosenbusch, L. Schweikhard, F. Wienholtz, R.N. Wolf, K. Zuber, Precision electron-capture energy in  $^{202}\text{Pb}$  and its relevance for neutrino mass determination. *Eur. Phys. J. A* **53**(7), 153 (2017)

69. J.S.E. Wieslander, J. Suhonen, T. Eronen, M. Hult, V.-V. Elomaa, A. Jokinen, G. Marissens, M. Misiaszek, M.T. Mustonen, S. Rahaman, C. Weber, J. Äystö, Smallest known  $q$  value of any nuclear decay: The rare  $\beta^-$  decay of  $^{115}\text{In}(9/2^+) \rightarrow ^{115}\text{Sn}(3/2^+)$ . *Phys. Rev. Lett.* **103**, 122501 (2009)

70. D.J. Wineland, H.G. Dehmelt, Principles of the stored ion calorimeter. *J. Appl. Phys.* **46**(2), 919–930 (1975)

71. M. Wurm, J.F. Beacom, L.B. Bezrukov, D. Bick, J. Blümer, S. Choubey, C. Ciemniak, D. D'Angelo, B. Dasgupta, A. Derbin, A. Dighe, G. Domogatsky, S. Dye, S. Eliseev, T. Enqvist, A. Erykalov, F. von Feilitzsch, G. Fiorentini, T. Fischer, M. Göger-Neff, P. Grabmayr, C. Hagner, D. Hellgartner, J. Hissa, S. Horiuchi, H.-T. Janka, C. Jaupart, J. Jochum, T. Kalliokoski, A. Kayunov, P. Kuusiniemi, T. Lachenmaier, I. Lazanu, J.G. Learned, T. Lewke, P. Lombardi, S. Lorenz, B. Lubsandorzhiev, L. Ludhova, K. Loo, J. Maalampi, F. Mantovani, M. Marafini, J. Maricic, T. Marrodán Undagoitia, W.F. McDonough, L. Miramonti, A. Mirizzi, Q. Meindl, O. Mena, R. Möllenbergs, V. Muratova, R. Nahnhauer, D. Nesterenko, Y.N. Novikov, G. Nuijten, L. Oberauer, S. Pakvasa, S. Palomares-Ruiz, M. Pallavicini, S. Pascoli, T. Patzak, J. Peltoniemi, W. Potzel, T. Räihä, G.G. Raffelt, G. Ranucci, S. Razzaque, K. Rummukainen, J. Sarkamo, V. Sinev, C. Spiering, A. Stahl, F. Thorne, M. Tippmann, A. Tonazzo, W.H. Trzaska, J.D. Vergados, C. Wiebusch, J. Winter, The next-generation liquid-scintillator neutrino observatory LENA. *Astropart. Phys.* **35**(11), 685–732 (2012)

72. V.A. Zheltonozhsky, A.M. Savrasov, N.V. Strilchuk, Tretyak *EPL. Europhys. Lett.* **121**(1), 12001 (2018)

73. K. Zuber, *Neutrino Physics*, 3rd edn. (CRC Press, Boca Raton, 2020)